

Synthesis and properties of the heterodinuclear complexes $[\text{Cp}(\text{CO})_2\text{Fe}(\text{CH}_2)_n\text{Ru}(\text{CO})_2\text{Cp}]$ (where $n = 3-6$; $\text{Cp} = \eta^5\text{-C}_5\text{H}_5$)

Steve J. Archer, Karol P. Finch, Holger B. Friedrich, John R. Moss*

Department of Chemistry, University of Cape Town, Rondebosch 7700 (South Africa)

and Andrew M. Crouch

School of Science, Peninsula Technikon, Bellville 7535 (South Africa)

(Received October 10, 1990)

Abstract

The new heterodinuclear complexes $[\text{Cp}(\text{CO})_2\text{Fe}(\text{CH}_2)_n\text{Ru}(\text{CO})_2\text{Cp}]$ (where $n = 4-6$ and $\text{Cp} = \eta^5\text{-C}_5\text{H}_5$) have been prepared by the reaction of the appropriate iodoalkyl compounds $[\text{CpFe}(\text{CO})_2(\text{CH}_2)_n\text{I}]$ with $\text{Na}[\text{CpRu}(\text{CO})_2]$. The compounds have been fully characterized by microanalysis, IR, ^1H NMR, ^{13}C NMR and mass spectroscopy. New data are also reported for the compound where $n = 3$. The spectroscopic data for the series of compounds where $n = 3-6$ are discussed. The thermal behaviour of the heterodinuclear compounds where $n = 3-5$ has been investigated by differential scanning calorimetry and the data are compared with those obtained for their homometallic analogues. A single crystal X-ray diffraction study on $[\text{Cp}(\text{CO})_2\text{Fe}(\text{CH}_2)_6\text{Ru}(\text{CO})_2\text{Cp}]$ confirms the presence of the zigzag hexamethylene chain with the metal atoms occupying terminal positions, but due to metal atom disorder in the crystal, accurate bond lengths and angles could not be obtained.

Introduction

It has been discovered that a catalyst containing more than one metal often has superior catalytic properties to either of its metallic components individually. This finding has been purported to rank as one of the most important discoveries in heterogeneous catalysis in the last 20 years [1] and has resulted in much effort being directed towards the synthesis and study of heterobimetallic compounds which could be used as catalysts themselves [2], catalyst precursors [3, 4] or as model compounds for catalytic intermediates [5–7].

Haloalkyl compounds have been used previously as precursors for heterodinuclear compounds [8] and the general importance of this approach has been shown subsequently [9]. We now describe how this route can be used to prepare new iron/ruthenium compounds. These compounds are of particular interest to us, since both Fe and Ru are active Fischer Tropsch catalysts. The comparison of spectroscopic data for the series of heterodinuclear compounds, which only differ in the number of methylene groups separating the two metals, is important because it

can yield information concerning the effect that one metal has on the other within the same molecule.

In order to obtain some quantitative information concerning the thermal behaviour of these heterodinuclear compounds, which may well be significant to termination processes in catalytic reactions, the compounds have been studied by differential scanning calorimetry (DSC). These results are compared with the DSC results previously reported for the di-iron compounds $[\text{Cp}(\text{CO})_2\text{Fe}(\text{CH}_2)_n\text{Fe}(\text{CO})_2\text{Cp}]$ ($n = 3-5$) [10] and with those now obtained for the di-ruthenium compounds $[\text{Cp}(\text{CO})_2\text{Ru}(\text{CH}_2)_n\text{Ru}(\text{CO})_2\text{Cp}]$ ($n = 3-5$).

Experimental

All reactions were carried out using standard Schlenk tube techniques under an atmosphere of nitrogen. THF was distilled over sodium wire. ^1H and ^{13}C NMR spectra were recorded on a Varian VXR 200 spectrometer. Chemical shifts are reported relative to tetramethylsilane ($\delta = 0.00$ ppm) as an external reference standard. NMR assignments were made with the aid of COSY and HETCOR experiments. IR spectra were recorded on a Perkin-Elmer

*Author to whom correspondence should be addressed.

983 spectrophotometer. Differential scanning calorimetry was performed on a Du Pont 910 DSC instrument and a Du Pont 990 thermal analyser; samples were heated in hermetically sealed pans in air. The low resolution mass spectra were recorded on a VG Micromass 16F spectrometer, operating at 70 eV or a Finnigan quadrupole spectrometer. Microanalyses were performed by the micro-analytical laboratory at the University of Cape Town. Melting points (m.p.) were determined on a Kofler hot-stage microscope (Reichert Thermovar) and are uncorrected. The compounds [CpRu(CO)₂]₂ [11], [CpFe(CO)₂]₂[μ-(CH₂)_n] (*n* = 3–6) [12, 13], [CpRu(CO)₂]₂[μ-(CH₂)_n] (*n* = 3–6) [14, 15], [Cp(CO)₂Fe(CH₂)₃Ru(CO)₂Cp] (1) [14] and [Cp(CO)₂Fe{(CH₂)_nI}] (*n* = 4–6) [16] were prepared by reported methods.

Preparation of [Cp(CO)₂Fe(CH₂)_nRu(CO)₂Cp], *n* = 4–6

A solution of Na[Cp(CO)₂Ru] (1.20 mmol) in THF (4 ml) was added while stirring to a solution of [Cp(CO)₂Fe{(CH₂)_nI}] (*n* = 4, 5 or 6) (0.86 mmol) in THF (3 ml) at –78 °C. The solution was allowed to attain room temperature and stirred for 48 h. The solvent was removed under reduced pressure, leaving an orange oily solid. The product was extracted with CH₂Cl₂ and the solvent then removed under reduced pressure. The resulting residue was dissolved in a minimum of hexane and chromatographed on a deactivated alumina column, eluting with hexane. A broad yellow band was collected. The resulting solution was concentrated under reduced pressure, filtered and cooled to –78 °C, when yellow crystals of the product precipitated. In this way the following compounds were prepared.

[Cp(CO)₂Fe(CH₂)₄Ru(CO)₂Cp] (2) (crude yield 46%, recrystallized yield 26%); m.p. 131–132 °C; IR (hexane): 2018(s), 2008(s), 1959(vs) cm⁻¹; ¹H NMR δ(CDCl₃): 5.22 (5H, s, CpRu), 4.71 (5H, s, CpFe), 1.66 (2H, s, RuCH₂), 1.54 (2H, s, RuCH₂CH₂), 1.50 (4H, s, FeCH₂CH₂); *m/z* 456 (*M*⁺). *Anal.* Found: C, 48.00; H, 4.10. Calc. for C₁₈H₁₈O₄FeRu: C, 47.48; H, 3.99%.

[Cp(CO)₂Fe(CH₂)₅Ru(CO)₂Cp] (3) (77%); m.p. 75–77 °C; IR (hexane): 2018(s), 2008(s), 1958(vs) cm⁻¹; ¹H NMR δ(CDCl₃): 5.23 (5H, s, CpRu), 4.73 (5H, s, CpFe), 1.64 (2H, m, RuCH₂–), 1.54 (2H, m, RuCH₂CH₂–), 1.44 (4H, s, Fe–CH₂CH₂–), 1.30 (2H, m, Fe–CH₂CH₂CH₂–); *m/z* 470 (*M*⁺). *Anal.* Found: C, 48.70; H, 4.40. Calc. for C₁₉H₂₀O₄FeRu: C, 48.63; H, 4.30%.

[Cp(CO)₂Fe(CH₂)₆Ru(CO)₂Cp] (4) (50%); m.p. 90–92 °C; IR (hexane): 2018(s), 2008(s), 1957(vs) cm⁻¹; ¹H NMR δ(CDCl₃): 5.16 (5H, s, CpRu), 4.66

(5H, s, CpFe), 1.67 (2H, m, RuCH₂–), 1.54 (2H, m, RuCH₂CH₂–), 1.45 (2H, s, FeCH₂CH₂–), 1.44 (2H, s, FeCH₂–), 1.31s (2H, s, FeCH₂CH₂CH₂–), 1.30 (2H, s, RuCH₂CH₂CH₂–); *m/z* 484 (*M*⁺). *Anal.* Found: C, 49.40; H, 4.60. Calc. for C₂₀H₂₂O₄FeRu: C, 49.68; H, 4.55%.

X-ray analysis

Single crystals of [Cp(CO)₂Fe(CH₂)₆Ru(CO)₂Cp] were obtained by slow crystallization of a dilute hexane solution at –15 °C. The X-ray analyses were carried out on an Enraf-Nonius diffractometer, using Mo Kα (λ = 0.7107 Å) radiation. Cell parameters were obtained from least-squares analysis of the setting angles of 24 reflections in the range 16° < θ < 17°. During data collection, the intensities of three reference reflections were monitored every hour and recentering was checked after every 100 measured reflections. Data were Lp processed and empirical absorption corrections applied [17]. Crystal data and other experimental data are given in Table 1.

Structure solution

The positions of the heavy atoms were found from a Patterson map in the space group *P*2₁/*c* with *Z* = 2. The structure was found to be disordered, with the

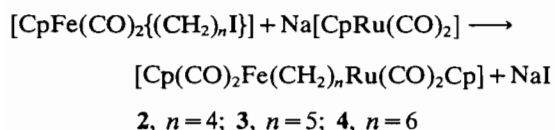
TABLE 1. Crystal data and parameters for data collection and refinement for [Cp(CO)₂Fe(CH₂)₆Ru(CO)₂Cp]

<i>Crystal data</i>	
Molecular formula	C ₂₀ H ₂₂ FeO ₄ Ru
Space group	<i>P</i> 2 ₁ / <i>c</i>
<i>a</i> (Å)	7.836(2)
<i>b</i> (Å)	10.358(2)
<i>c</i> (Å)	12.615(2)
β (°)	98.21(2)
<i>V</i> (Å ³)	1013
<i>D</i> _c for <i>Z</i> = 2 (g cm ⁻³)	1.58
<i>F</i> (000)	488
<i>Data collection</i>	
μ(Mo Kα) (cm ⁻¹)	13.7
Crystal dimensions (mm)	0.35 × 0.52 × 0.48
Crystal decay (%)	1.3
Scan mode	ω–2θ
Scan width (°ω)	(0.85 + 0.35 tan θ)
Aperture width (mm)	(1.12 + 1.05 tan θ)
θ Range scanned (°)	1–25
<i>Refinement</i>	
No. reflections collected	1784
No. reflections observed	
(with <i>I</i> _{rel} > 2σ <i>I</i> _{rel})	1579
No. parameters	167
<i>R</i> = Σ <i>F</i> _o – <i>F</i> _c /Σ <i>F</i> _o	0.055
<i>R</i> _w = Σ <i>w</i> ^{1/2} <i>F</i> _o – <i>F</i> _c /Σ <i>w</i> ^{1/2} <i>F</i> _o	0.049
Weighting scheme	5.81(σ ² <i>F</i>) ⁻¹

asymmetric unit being $\text{Cp}(\text{CO})_2(\text{Ru}/\text{Fe})(\text{CH}_2)_3$. The centre of the molecule lay at a special position. The cyclopentadienyl ring exhibited orientational disorder, with relative populations being 80:20. Other details of the final refinement are given in Table 1. See also 'Supplementary material'. The structure was solved using SHELX76 [18]. Complex neutral atom scattering factors were taken from Cromer and Mann [19] and dispersion correction from Cromer and Liberman [20]. PLUTO produced the drawings [21].

Results and discussion

The new heterodinuclear compounds were prepared by the reaction of the appropriate iodoalkyl compound with $\text{Na}[\text{CpRu}(\text{CO})_2]$ according to the equation



The products were characterized by microanalysis, ^1H NMR, ^{13}C NMR, IR and mass spectroscopy (see Tables 2 and 3 and 'Experimental').

We now report and discuss the spectroscopic data for the four heterobinuclear compounds $[\text{Cp}(\text{CO})_2\text{Fe}(\text{CH}_2)_n\text{Ru}(\text{CO})_2\text{Cp}]$ ($n = 3-6$), and compare these data with those of their monometallic analogues.

IR spectra

The heterobinuclear compounds **1-4** all show three bands in the $\nu(\text{CO})$ region in hexane solution. For example, **2** shows bands at 2018(s) (which can be assigned to $\text{Ru}-\text{CO}$), 2008(s) ($\text{Fe}-\text{CO}$) and 1959 (vs) (both $\text{Ru}-\text{CO}$ and $\text{Fe}-\text{CO}$) cm^{-1} . These assignments were made by comparing the data found for the monometallic analogues [12, 14]. The data suggest that each metal unit is essentially independent of the other and that there is no coupling of CO vibrations. There is little change in $\nu(\text{CO})$ with increasing methylene chain length in compounds **1-4**.

Mass spectra

Mass spectrometry is the simplest readily available method to unambiguously confirm the composition of these heterodinuclear complexes, since all other spectral data obtained do not completely exclude the possible presence of equimolar quantities of the homodinuclear alkanediyl complexes of the respective transition metals. Thus the heterobimetallic nature of these complexes is confirmed either by the observation of a molecular ion for the proposed structure or fragment ions which are only possible from the heterodinuclear complex.

Compounds **1-4** all show weak molecular ions (c. 1%) in their mass spectra. The major ions observed in the electron impact mass spectra of compounds **1-4** are listed in Table 2. Because the masses of CO and Fe are both multiples of 14 (the mass of one CH_2 unit) many mass spectral assignments are ambiguous and the exact fragmentation sequence is not certain from the low resolution data obtained. However, often the exact order of fragment loss is not significant and in many cases other data available indicates which of two possible assignments is the more likely. The possible fragmentation sequences giving rise to these ions are very similar to those observed for the complexes $[\text{Cp}(\text{CO})_2\text{Fe}(\text{CH}_2)_n\text{ML}_y]$ ($n = 3-6$; $\text{ML}_y = \text{Mo}(\text{CO})_3\text{Cp}$, $\text{W}(\text{CO})_3\text{Cp}$) shown in the scheme in ref. 9.

Ions corresponding to $[\text{Cp}_2\text{Fe}]^+$ and $[\text{Cp}_2\text{Ru}]^+$ are observed in all the spectra. The formation of ferrocene in complexes containing the $[\text{Cp}(\text{CO})_2\text{Fe}]$ unit has been observed previously [9, 16, 22] and it is of interest to observe that the $[\text{Cp}(\text{CO})_2\text{Ru}]$ complexes behave similarly. The ions $[\text{CpRu}(\text{CO})_x]^+$ ($x = 0-2$) are relatively abundant and thus also comparable with their Fe analogs ($[\text{CpFe}(\text{CO})_x]^+$ ($x = 0-2$)). $[\text{CpFe}]^+$ (m/z 121) is the base peak in all these spectra.

Ions involving metal-metal bonding after loss of the methylene bridge are relatively abundant, even though the expected precursor, $[\text{Cp}(\text{CO})_2\text{FeRu}(\text{CO})_2\text{Cp}]^+$ is not observed unambiguously. The ion representing $[\text{CpFeRuCp}]$ is most abundant in the cases where $n = 3$ and progressively decreases in relative intensity as the methylene chain lengthens to $n = 6$. This indicates a stronger interaction between Fe and the atom at the other end of the carbon chain (Ru in this case) for shorter chain complexes. Similar behaviour was observed in the mass spectra of the complexes $[\text{Cp}(\text{CO})_2\text{Fe}\{(\text{CH}_2)_n\text{X}\}]$ ($n = 3-10$; $\text{X} = \text{I}, \text{Br}$) [16] and $[\text{Cp}(\text{CO})_2\text{Fe}(\text{CH}_2)_n\text{ML}_y]$ ($n = 3-6$; $\text{ML}_y = \text{Mo}(\text{CO})_3\text{Cp}$, $\text{W}(\text{CO})_3\text{Cp}$, $\text{Re}(\text{CO})_5$) [9]. In all the spectra, the ion corresponding to $[\text{FeRu}]^+$ is not observed.

The loss of C_5H_5 (65 dalton) is not usually observed in the mass spectral fragmentation of compounds **1-4**. In contrast, the loss of C_5H_6 (66 dalton) does seem to occur, not from the molecular ion itself, but after the initial loss of 2 or more carbonyls from the molecular ion.

It is interesting to note that complexes **1-4** appear to retain their heterobimetallic nature in most of the major fragmentation routes.

^1H NMR spectra

The ^1H NMR spectra of **2-4** compare well with that reported for **1** [14]. Two separate Cp resonances

TABLE 2. Mass spectral data for complexes $[\text{Cp}(\text{CO})_2\text{Fe}(\text{CH}_2)_n\text{Ru}(\text{CO})_2\text{Cp}]$

Ions (singly charged positive)	Relative intensity of ion ^a (% of base peak)			
	<i>n</i> = 3	<i>n</i> = 4	<i>n</i> = 5	<i>n</i> = 6
<i>m</i> ^b	< 1	2	1	(CI) ^c
<i>m</i> -(CH ₂) _{<i>n</i>}	0	2 ^d	0	0
<i>m</i> -CO	0	2	0	0
<i>m</i> -2CO	< 1	2	< 5	1
<i>m</i> -3CO	0	10 ^d	3	0
<i>m</i> -4CO	3	10 ^d	< 2	10 ^d
<i>m</i> -2CO-(CH ₂) _{<i>x</i>} ^e	Ion intensity ≤ 1% except for ions also representing [<i>m</i> -(CH ₂) _{<i>n</i>} -(CO) _{<i>x</i>}] ^{+f}			
<i>m</i> -(CH ₂) _{<i>n</i>} -CO	14	12	20	12
<i>m</i> -(CH ₂) _{<i>n</i>} -2CO	9	9	12	2
<i>m</i> -(CH ₂) _{<i>n</i>} -3CO	7	9	9	6
<i>m</i> -(CH ₂) _{<i>n</i>} -4CO	31	22	23	10
<i>m</i> -2CO-CpH	0	10	23	10
<i>m</i> -3CO-CpH	5	15	28	13
<i>m</i> -4CO-CpH ^g	16	40	18	12
<i>m</i> -2CO-CpH-(CH ₂) _{<i>x</i>} ^e	Ion intensity ≤ 10% except for values corresponding to above ions			
<i>m</i> -Cp(CO) ₂ Fe-(14) ₂ ^h	0	85	17	15
<i>m</i> -Cp(CO) ₂ Fe-(14) ₃	59	0	12	5
<i>m</i> -Cp(CO) ₂ Fe-(14) ₄	17	75	12	15
<i>m</i> -Cp(CO) ₂ Fe-(14) ₅	30	0	24	0
<i>m</i> -Cp(CO) ₂ Fe-(14) ₆	1	40	0	3
<i>m</i> -Cp(CO) ₂ Fe-(14) ₇	53	0	25	0
<i>m</i> -Cp(CO) ₂ Fe-(14) ₈	— ⁱ	72	0	35
<i>m</i> -Cp(CO) ₂ Fe-(14) ₉	—	—	45	0
<i>m</i> -Cp(CO) ₂ Fe-(14) ₁₀	—	—	—	85
<i>m</i> -Cp(CO) ₂ Fe-(14) ₁₁	—	—	—	—
<i>m</i> -Cp(CO) ₂ Fe-(14) ₁₂	—	—	—	—
[RuC ₃ H ₃]	8	8	8	< 1
Cp(CO) ₂ Fe(CH ₂) _{<i>n</i>}	0	2	20	20
Cp(CO) ₂ Fe(CH ₂) _{<i>n</i>} -(14) ₂ ^j	0	28	80	80
Cp(CO) ₂ Fe(CH ₂) _{<i>n</i>} -(14) ₃	15	0	8	3
Cp(CO) ₂ Fe(CH ₂) _{<i>n</i>} -(14) ₄	30	30	20	15
Cp(CO) ₂ Fe(CH ₂) _{<i>n</i>} -(14) ₅	23	—	23	0
Cp(CO) ₂ Fe(CH ₂) _{<i>n</i>} -(14) ₆	4	30	3	5
Cp(CO) ₂ Fe(CH ₂) _{<i>n</i>} -(14) ₇	100	—	30	—
Cp(CO) ₂ Fe(CH ₂) _{<i>n</i>} -(14) ₈	—	100	0	40
Cp(CO) ₂ Fe(CH ₂) _{<i>n</i>} -(14) ₉	—	—	100	—
Cp(CO) ₂ Fe(CH ₂) _{<i>n</i>} -(14) ₁₀	—	—	—	100
Cp(CO) ₂ Fe(CH ₂) _{<i>n</i>} -(14) ₁₁	—	—	—	—
[FeC ₃ H ₃]	4	10	10	10
Fe	28	36	34	70
Ru	21	3	1	3
Cp ₂ Fe	15	24	38	15
Cp ₂ Ru	33	32	54	84
FeCpRu	Equivalent to [CpRu(CO) ₂] ⁺			

^aIon intensity listed is that of the most abundant isotope combination. ^b*m* = Cp(CO)₂Fe(CH₂)_{*n*}Ru(CO)₂Cp. ^c(CI) = molecular ion evident in chemical ionization spectrum only. ^dIon has more than one possible assignment; another assignment is more probable. ^e(CH₂)_{*x*}; 2 ≤ *x* ≤ *n*. ^f(CO)_{*x*}; *x* = 1–4. ^g[*m*-4CO-CpH]⁺ is numerically equivalent to [*m*-Cp(CO)₂FeH]⁺. ^hIons at these masses could be due to any appropriate losses of CH₂ and CO; the final species after the series of losses is [CpRu]⁺. ⁱIon not applicable to this complex. ^jIons at these masses could be due to any appropriate combination of losses of CH₂ and CO; the final species after the series of losses is [CpFe]⁺.

can readily be assigned to CpRu and CpFe. We have also resolved and assigned the methylene resonances (see 'Experimental').

¹³C NMR spectra

¹³C NMR data and assignments for compounds **1** and [Cp(CO)₂Ru(CH₂)_{*n*}Ru(CO)₂Cp] (*n* = 3 or 4)

have been previously reported [14], however, some of this data appears to be incorrect. We now report ¹³C NMR data and assignments for all the compounds [Fp(CH₂)_{*n*}Fp], [Rp(CH₂)_{*n*}Rp] and [Fp(CH₂)_{*n*}Rp] (*n* = 3–6; Fp = CpFe(CO)₂; Rp = CpRu(CO)₂) in Table 3. From these data it can be seen that the chemical shifts of neither the carbonyl nor Cp peaks

TABLE 3. ^{13}C NMR data for the alkanediyl compounds^a

n	$\text{Cp}(\text{CO})_2\text{Fe}(\text{CH}_2)_n\text{Fe}(\text{CO})_2\text{Cp}$ Fe-CO	Fe- CH_2	Fe- CH_2 - CH_2	Fe- CH_2 - CH_2 - CH_2					
3 ^b	217.9	85.2	7.8	47.4					
4 ^b	217.8	85.4	3.8	43.8					
5	217.8	85.3	4.0	38.3					
6	217.7	85.3	3.8	38.3					
n	$\text{Cp}(\text{CO})_2\text{Ru}(\text{CH}_2)_n\text{Ru}(\text{CO})_2\text{Cp}$ Ru-CO	Ru- CH_2	Ru- CH_2 - CH_2	Ru- CH_2 - CH_2 - CH_2					
3	202.6	88.5	0.9	50.1					
4 ^c	202.5	88.6	-3.3	45.2					
5 ^d	202.5	88.5	-3.0	39.7					
6 ^e	202.5	88.5	-3.2	39.9					
n	$\text{Cp}(\text{CO})_2\text{Fe}(\text{CH}_2)_n\text{Ru}(\text{CO})_2\text{Cp}$ Fe-CO	Ru-CO	Fe-Cp	Ru- CH_2	Fe- CH_2	Fe- CH_2 - CH_2	Ru- CH_2 - CH_2 - CH_2	Ru- CH_2 - CH_2 - CH_2 - CH_2	Fe- CH_2 - CH_2 - CH_2 - CH_2
3	217.9	202.6	88.5	85.2	1.0	7.7	48.7		
4	217.8	202.5	88.6	85.3	-3.2	3.7	43.8	45.2	
5	217.8	202.5	88.6	85.3	-3.0	4.1	38.2	39.7	
6	217.8	202.5	88.6	85.3	-3.2	3.9	38.4	39.9	
								40.2	
								34.4	
								34.5	

^aMeasured in CDCl_3 , peaks externally referenced to TMS (0.0 ppm). ^bData from ref. 24. ^cData from ref. 14 (but new assignments have been made, see text).^dData from ref. 15. ^eData from ref. 15 (but new assignments have been made).

of these nine complexes vary significantly. As one would expect, the methylene carbon α to a metal is influenced most strongly by that metal. Noteworthy is the shift of approximately 4 ppm in the chemical shift of the α carbon atom as the chain length increases from $n=3$ to $n=4$ or longer. It is possible that each of the α carbons in the complex where $n=3$ still feels an effect due to the metal on the other end of the chain. The β carbon chemical shift of complex **1** is in an intermediary position to the positions of the β carbon chemical shifts of $[\text{Fp}(\text{CH}_2)_3\text{Fp}]$ and $[\text{Rp}(\text{CH}_2)_3\text{Rp}]$, suggesting that the two different metals of **1** influence the β carbon equally. For complex **2** the chemical shifts of the carbons α and β to a particular metal are very similar or identical to their homometallic analogues. The same applies in compounds **3** and **4** for the α , β and γ carbon atoms.

DSC data

μ -Alkanediyl complexes can be used as models for hydrocarbon fragments interacting with two active metal sites on a catalyst surface. Decomposition studies of these complexes are thus relevant to chain termination processes in catalytic reactions. We have used differential scanning calorimetry to obtain some quantitative information about the decomposition of the heterodinuclear alkanediyl complexes. Previously, we have reported results of a DSC study (up to 230 °C) of the di-iron complexes $[\text{Fp}(\text{CH}_2)_n\text{Fp}]$ ($n=3-12$) [10]. The DSC data for the compounds $[\text{Fp}(\text{CH}_2)_n\text{Fp}]$, $[\text{Rp}(\text{CH}_2)_n\text{Rp}]$ and $[\text{Fp}(\text{CH}_2)_n\text{Rp}]$ (where $n=3-5$) are summarized in Table 4. All of the compounds show a sharp endotherm at low temperature that corresponds to the melting point (m.p.) of the compound. We notice also that the m.p.s of the mixed metal compounds are very close to the m.p.s of the di-ruthenium compounds. For the three series, the m.p.s of the compounds where $n=4$ are higher than the m.p.s of either $n=3$ or 5. Also, the m.p.s tend

to decrease with increasing chain length as found for the more extensive series $[\text{Fp}(\text{CH}_2)_n\text{Fp}]$ (where $n=3-12$) [10].

For the compounds $[\text{Fp}(\text{CH}_2)_n\text{Fp}]$ (where $n=3-5$), we assign the first T_{max} exotherm (exo) to decomposition which results in the loss of the hydrocarbon chain, as has been reported previously and confirmed by identifying the organic decomposition products [10, 14]. The compound $[\text{Fp}(\text{CH}_2)_n\text{Fp}]$, where $n=3$, decomposes at the lowest temperature compared to the di-iron compounds where $n=4$ or 5. The second T_{max} endotherm (endo) for the compounds $[\text{Fp}(\text{CH}_2)_n\text{Fp}]$ is probably due to the decomposition of $[\text{CpFe}(\text{CO})_2]_2$ which has T_{max} endo at 285 °C under these conditions.

For the compounds $[\text{Rp}(\text{CH}_2)_n\text{Rp}]$, the first T_{max} exo, which we believe to be due to decomposition, occurs at the highest temperature for $[\text{Rp}(\text{CH}_2)_3\text{Rp}]$ (221 °C) when compared with the tetra- and pentamethylene bridged di-ruthenium compounds. This shows an opposite trend to that for the di-iron analogues. Thus the mechanism of decomposition of the trimethylene compounds may be metal dependent. That different decomposition mechanisms are operative for $[\text{Fp}(\text{CH}_2)_3\text{Fp}]$ and $[\text{Rp}(\text{CH}_2)_3\text{Rp}]$ is further borne out by the differing ratios of propene:cyclopropane observed on decomposition. Thus, decomposition of $[\text{Fp}(\text{CH}_2)_3\text{Fp}]$ gives mainly cyclopropane and decomposition of $[\text{Rp}(\text{CH}_2)_3\text{Rp}]$ gives mainly propene, whereas the decomposition behaviour of $[\text{Fp}(\text{CH}_2)_3\text{Rp}]$ lies somewhere between the two [10, 14]. The DSC results support this with the first T_{max} exo for $[\text{Fp}(\text{CH}_2)_3\text{Rp}]$ (at 174 °C) which lies midway between that for $[\text{Fp}(\text{CH}_2)_3\text{Fp}]$ (143 °C) and $[\text{Rp}(\text{CH}_2)_3\text{Rp}]$ (221 °C). For compounds $[\text{Rp}(\text{CH}_2)_n\text{Rp}]$ (where $n=3-5$) another T_{max} exo is seen in the range 248–284 °C which can be ascribed to further decomposition.

TABLE 4. DSC data for alkanediyl complexes (°C)^a

$n =$	$\text{Fp}(\text{CH}_2)_n\text{Fp}$			$\text{Rp}(\text{CH}_2)_n\text{Rp}$			$\text{Fp}(\text{CH}_2)_n\text{Rp}$		
	3	4	5	3	4	5	3	4	5
Melting point ^b	104–105	112–115 (125–126)	83–85	84–87	131–132	77–84	85–86	131–132	75–77
T_{max} endo	105	115 (128)	85	91	138	86	94	126	78
T_{max} exo	143	160	158	221	177	156	174	163	174
T_{max} endo	283	271	290						
T_{max} exo				277	248	284	311 386	325 435	320 386

^a $\text{Fp} = \text{CpFe}(\text{CO})_2$, $\text{Rp} = \text{CpRu}(\text{CO})_2$. ^bDetermined on a Kofler hot-stage microscope.

For the compounds $[\text{Fp}(\text{CH}_2)_n\text{Rp}]$, the first T_{max} exo shows little variation with chain length (174, 163 and 174 °C for $n=3-5$, respectively). Thus, the apparent easy decomposition pathway for $[\text{Fp}(\text{CH}_2)_3\text{Fp}]$ does not appear accessible for $[\text{Fp}(\text{CH}_2)_3\text{Rp}]$ or $[\text{Rp}(\text{CH}_2)_3\text{Rp}]$. The final T_{max} exo for the mixed metal dimers are higher than those for either of the homometallic species and a second T_{max} exo is also observed. The DSC data for the mixed metal dimers are different to either of the monometallic dimers but the overall behaviour is closer to that of $[\text{Rp}(\text{CH}_2)_3\text{Rp}]$. This suggests that the mixed metal compounds retain their heterobimetallic character during decomposition and do not decompose to homometallic species; they may well yield Fe/Ru decomposition products, e.g. $[\text{FpRp}]$. This suggests that the decomposition pathways are intramolecular rather than intermolecular.

The implied consequences of this behaviour for catalysis are that a catalyst derived from a heterodinuclear compound may well lead to *different* species on decomposition than would be obtained from a mixture of the homometallic analogues. Thus heterodinuclear compounds may be good precursors for new types of mixed metal catalysts.

X-ray diffraction study of compound 4

The structure of compound 4 was determined by X-ray diffraction. Unfortunately the single crystals that were obtained were disordered. The extent of the disorder in this structure allows nothing but the gross conformation of the molecule to be described (Fig. 1). As in other structures of alkanediyl complexes, the two metals are connected by a zigzag alkyl chain [15, 23, 24]. As necessitated by the centre of symmetry within the molecule, the Cp rings and CO groups lie on opposite sides of the molecule. This is also observed in the structures of $[\text{Cp}(\text{CO})_2\text{Fe}(\text{CH}_2)_n\text{Fe}(\text{CO})_2\text{Cp}]$ ($n=3, 4$) [24], but not in those of $[\text{Cp}(\text{CO})_2\text{Ru}(\text{CH}_2)_3\text{Ru}(\text{CO})_2\text{Cp}]$ [15] and $[\text{Cp}(\text{CO})_2\text{FeC}(\text{O})(\text{CF}_2)_3\text{C}(\text{O})\text{Fe}(\text{CO})_2\text{Cp}]$ [25] where the Cp rings are on the same side of the molecule.

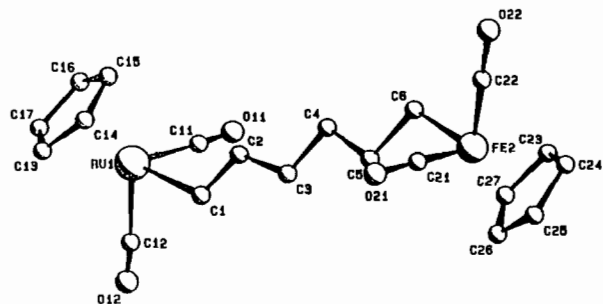


Fig. 1. Structure of compound 4.

We have found the same type of disorder of the Fe/Ru atoms in the complex $[\text{Cp}(\text{CO})_2\text{FeCH}_2\text{-CHCH}_2\text{Ru}(\text{CO})_2\text{Cp}]^+\text{PF}_6^-$ [26], whilst this disorder has also recently been reported in another 'symmetrical' Fe/Ru complex, $[\text{FeRu}(\text{CO})_8]^{2-}$ [27]. The cause is clearly that the two ends of the molecules are virtually identical. In each case it may be argued that the lattice energies for the observed disordered structure and the hypothetical structure without disorder must be of the same order of magnitude. Maximization of entropy is then the driving force behind the occurrence of the mixed Fe/Ru structures, at least at -15 °C, under the conditions used for crystal formation. The disorder could presumably be avoided by altering the ligand system on one of the metal atoms; we are currently exploring this possibility.

Supplementary material

Tables of fractional atomic coordinates and observed and calculated structure factors for compound 4 (11 pages) are available from the authors on request.

Acknowledgements

We thank Johnson Matthey Ltd. and PGM Chemicals for generous loans of ruthenium trichloride and the University of Cape Town, FRD and Chamber of Mines for support. We also thank Mr N. Ahmed for the preparation of $[\text{CpRu}(\text{CO})_2]_2$, Mr P. A. Makhsha for preparing some haloalkyl iron complexes, and Ms B. K. Williamson and Mr G. Grierson (Rembrandt International) for running the mass spectra.

References

- 1 R. D. Adams, *Polyhedron*, 7 (1988) 2251, and refs. therein.
- 2 Z. T. Horrath, M. Garland, G. Bor and P. Pino, *J. Organomet. Chem.*, 358 (1988) C17.
- 3 J. R. Budge, J. P. Scott and B. C. Gates, *J. Chem. Soc., Chem. Commun.*, 342 (1983).
- 4 A. Fukuoka, T. Kimura and M. Ichikawa, *J. Chem. Soc., Chem. Commun.*, (1988) 428.
- 5 E. N. Jacobsen, K. I. Goldberg and R. G. Bergman, *J. Am. Chem. Soc.*, 110 (1988) 3706.
- 6 F. Ozawa, J. W. Park, P. B. Mackenzie, W. P. Schaefer, L. M. Henling and R. H. Grubbs, *J. Am. Chem. Soc.*, 111 (1989) 1319.
- 7 I. J. Hart, J. C. Jeffery, R. M. Lowry and F. G. A. Stone, *Angew. Chem., Int. Ed. Engl.*, 27 (1988) 1703.
- 8 J. R. Moss, *J. Organomet. Chem.*, 231 (1982) 229.

- 9 H. B. Friedrich, J. R. Moss and B. K. Williamson, *J. Organomet. Chem.*, **394** (1990) 313.
- 10 J. R. Moss, L. G. Scott, M. E. Brown and K. J. Hindson, *J. Organomet. Chem.*, **282** (1985) 255.
- 11 N. M. Doherty and S. A. R. Knox, *Inorg. Synth.*, **25** (1989) 179.
- 12 R. B. King, *Inorg. Chem.*, **2** (1963) 531.
- 13 S. F. Mapolie and J. R. Moss, *Organomet. Synth.*, **4** (1988) 198.
- 14 M. Cooke, N. J. Forrow and S. A. R. Knox, *J. Chem. Soc., Dalton Trans.*, (1983) 2435.
- 15 K. P. Finch, J. R. Moss and M. L. Niven, *Inorg. Chim. Acta*, **166** (1989) 181.
- 16 H. B. Friedrich, P. A. Makhesha, J. R. Moss and B. K. Williamson, *J. Organomet. Chem.*, **384** (1990) 325.
- 17 A. C. T. North, D. C. Philips and F. S. Mathews, *Acta Crystallogr., Sect. A*, **24** (1968) 351.
- 18 G. M. Sheldrick, in H. Schenk, R. Olthof-Hazenkamp, H. van Koningsveld and G. C. Bassi (eds.), *Computing in Crystallography*, Delft University Press, Delft, 1978, pp. 34–42.
- 19 D. T. Cromer and J. B. Mann, *Acta Crystallogr., Sect. A*, **24** (1968) 321.
- 20 D. T. Cromer and D. Liberman, *J. Chem. Phys.*, **53** (1970) 1891.
- 21 W. D. S. Motherwell, *PLUTO*, program for plotting molecular and crystal structures, Cambridge University, U.K., 1974.
- 22 R. B. King, *J. Am. Chem. Soc.*, **90** (1968) 1417.
- 23 K. Raab, U. Nagel and W. Beck, *Z. Naturforsch., Teil B*, **38** (1983) 1466.
- 24 L. Pope, P. Sommerville, M. Laing, K. Hindson and J. R. Moss, *J. Organomet. Chem.*, **112** (1976) 309.
- 25 S. J. Archer *et al.*, manuscript in preparation.
- 26 S. J. Archer, H. B. Friedrich and J. R. Moss, unpublished results.
- 27 N. K. Battacharyya, T. J. Coffy, W. Quintane, T. A. Salupo, J. C. Bricker, T. B. Shay, M. Payne and S. G. Shore, *Organometallics*, **9** (1990) 2368.